Site-Directed Mutations Affecting the Spectroscopic Characteristics and Midpoint Potential of the Primary Donor in Photosystem I†

Andrew N. Webber,*,‡ Hui Su,‡ Scott E. Bingham,‡ Hanno Käss,§ Ludwig Krabben,§ Matthias Kuhn,§ Rafael Jordan,§ Eberhard Schlodder,§ and Wolfgang Lubitz§

Department of Botany and Center for the Study of Early Events in Photosynthesis, Arizona State University, Tempe, Arizona 85287-1601, and Max-Volmer-Institut für Biophysikalische und Physikalische Chemie, Technische Universität Berlin, Strasse d. 17. Juni 135, D-10623 Berlin, Germany

Received May 20, 1996; Revised Manuscript Received July 25, 1996⊗

ABSTRACT: Photosystem I is a member of the iron−sulfur center or type I reaction centers. The primary electron donor in photosystem I is a chlorophyll *a* dimer termed P_{700}. The biophysical properties of P_{700} are well understood, but the protein environment that gives it such unique properties is unknown. We have characterized site-directed mutants of the photosystem I reaction center protein PsaB and identified an amino acid, His-656, that interacts closely with one of the P_{700} chlorophylls. Mutation of His-656 to Asn or Ser increases the oxidation midpoint potential of $P_{700}/P_{700}^{+\bullet}$ by 40 mV. The $P_{700}/P_{700}^{+\bullet}$ optical difference spectra show the appearance of a new bleaching band at 667 nm. Electron nuclear double resonance spectroscopy indicates a significant increase in the hyperfine coupling corresponding to methyl protons at position 12 of the spin carrying chlorophyll *a* of $P_{700}^{+\bullet}$. The implication of these results to current structural models of the photosystem I reaction center is discussed.

Photosynthesis occurs in specialized pigment protein complexes termed reaction centers (RCs). The RC protein complexes of green sulfur bacteria, *Heliobacteria*, and photosystem I (PSI)[1] contain an iron−sulfur center serving as the terminal electron acceptor and are referred to as "iron−sulfur-type" or type I RCs. A mobile quinone is the terminal electron acceptor in purple bacteria and photosystem II (PSII) that are referred to as "quinone-type" or type II RCs. A detailed structure is available for the RC of purple bacteria (bRC) (Deisenhofer et al., 1984; Allen et al., 1987; Chang et al., 1991; Ermler et al., 1994). The primary electron donor is a special pair of bacteriochlorophyll *a* molecules (BChls) coordinated by a His residue from the L and M subunits of the bRC heterodimer. In PSI, the RC Chl (P_{700}) and early electron acceptors A_0, A_1, and F_X, are coordinated by a heterodimeric complex of two related proteins, PsaA and PsaB (Golbeck, 1992). Both PsaA and PsaB are predicted to span the thylakoid membrane 11 times (Fish et al., 1985a,b). A low-resolution structure of PSI derived from crystals refracting at 4.5 Å has been published, but little information on coordination of cofactors is available (Schubert et al., 1995). Spectroscopic and biochemical characterization of the bRC complexes of the green sulfur bacterium *Chlorobium limicola* (Büttner et al., 1992) and *Heliobacillus mobilis* (Liebl et al., 1993) has convincingly shown that they are very similar to PSI and that, as with the case of type II RCs, the type I RCs also share a common ancestor.

The primary electron donor in PSI (P_{700}) is a Chl *a* dimer thought to be coordinated by amino acids from both PsaA and PsaB (Golbeck, 1992). Spectroscopic analysis of $P_{700}^{+\bullet}$ in single crystals of PSI from *Synechococcus elongatus* indicates that the charge density distribution over the two dimer halves is highly asymmetric (Käss, 1995). This would indicate that the protein environment is critical in modulating the physicochemical properties of the P_{700} dimer. It is not known which regions of PsaA and PsaB are involved in coordinating the P_{700} dimer. It might be expected that regions important for PSI function will be conserved in the amino acid sequences of PsaA and PsaB from evolutionary diverse organisms as well as in the RC proteins from *Heliobacillus* and *Chlorobium*. Several amino acids and domains can be identified by comparison of amino acid sequences of PsaA, PsaB, and bRC proteins (Figure 1) (Büttner et al., 1992; Liebl et al., 1993). In particular, a region containing two cysteines now known to be involved in coordinating F_X is very conserved (Büttner et al., 1992; Liebl et al., 1993; Smart et al., 1993; Webber et al., 1993). A conserved histidine in the putative membrane span VIII domain has frequently been suggested to serve as a P_{700} ligand, but this has now been ruled out by spectroscopic analysis of site-directed mutants in *Chlamydomonas reinhardtii* (Cui et al., 1995). The helix X domain of PsaB has been shown to exhibit weak homology to the helix D domain of the D1 and D2 RC polypeptides of PSII (Marguilles, 1991). A histidine in this helix X domain (Figure 1), residue number 656 in PsaB of *C. reinhardtii*, is conserved in all sequences and has also been proposed as a candidate to ligate P_{700} (Marguilles, 1991; Vermaas, 1994; Fromme et al., 1994; Cui et al., 1995).

† This work was supported by the National Research Initiatives Competitive Grants Program of the USDA (95-37306-2044), Deutsche Forschungsgemeinschaft (TP A4 and A5, SFB 312), and NATO (CRG 950759).

* To whom correspondence should be addressed at the Department of Botany, Arizona State University, Box 871601, Tempe, AZ 85287-1601. Phone: (602) 965-8725. Fax: (602) 965-6899. E-mail: andrew.webber@asu.edu.

‡ Arizona State University.

§ Technische Universität Berlin.

⊗ Abstract published in *Advance ACS Abstracts,* September 1, 1996.

[1] Abbreviations: bp, base pair(s); Bchl *a*, bacteriochlorophyll *a*; Bpheo *a*, bacteriopheophytin *a*; Chl *a*, chlorophyll *a*; CP43, antenna complex of photosystem II core; ENDOR, electron nuclear double resonance; hfc, hyperfine coupling constant; hfi, hyperfine interaction; LHC, light harvesting complex; Phe *a*, pheophytin *a*; PSI, photosystem I; PSII, photosystem II; P_{680}, primary electron donor in PSII; P_{700}, primary electron donor in PSI; ν_{1H}, nuclear Larmor frequency of ^{1}H.

S0006-2960(96)01198-1 CCC: $12.00

```
                        VIII
H. mobilis      FVAAHAIAGGLHFTMVPLWRMVFFSKVSPWTTKVGMKAKRDGEFPCLGPAYGGTCSISLV
C. limicola     WVMAHVITAGSLFSLIALVRIAFFAHTSPLWDDLGLK KNSYSFPCLGPVYGGTCGVSIQ
S. 6803         FLVHHAIALGLHTTALILIKGALESRGSKLMPD...KKDFGYSFPCDGPGRGGTCDISAW
PsaB maize      FLVHHAIALGLHTTTLILVKGALDARGSKLMPD...KKDFGYSFPCDGPGRGGTCDISAW
PsaB cr         FLVHHAIALGLHTTTLILVKGALDARGSKLMPD...KKDFGYSFPCDGPGRGGTCDISAY
                519                                          FX

                        IX
H. mobilis      DQFYLAIFFSLQVIAPAWFYLDGCWMGSFVATSSEVYKQAAELFKANPTWFSLHAVSNFT
C. limicola     DQ..LW.FAMLWGIKGLSAVCWYIDGAWIASMMYGVPAADAKAWDSIA.....HLQH
S. 6803         DAFYLAMFWMLNTLGWLTFYWHWKHLGVWSGNVAQ.....FNENSTYLMGWFRD
PsaB maize      DAFYLAVFWMLNTIGWVTFYWHWKHITLWQGNVSQ.....FNESSTYLMGWLRD
PsaB cr         DAFYLAVFWMLNTIGWVTFYWHWKHLTLWQGNVAQ.....FDESSTYLMGWLRD
                576

                                        X
H. mobilis      SEVTSATSSLKPLVCSNTT.MVTWFKPCWAAHFIWAFTFSMLFQYRGSRD
C. limicola     HYTSGIFYYFWTETVTIF.SSSHLSTILMIGHLVWFISFAVWFEDRGSRL
S. 6803         YLWANSAQLINGYNPYGVNNLSVWAWMFLFGHLVWATGFMFLISWRGYWQ
PsaB maize      YLWLNSSQLINGYNPFGMNSLSVWAWMFLFGHLVWATGFMFLISWRGYWQ
PsaB cr         YLWLNSSQLINGYNPFGMNSLSVWAWTFLFGHLIYATGFMFLISWRGYWQ
                625
```

FIGURE 1: Amino acid sequences of the C-terminal region of reaction center protein from *H. mobilis* (Liebl et al., 1993) and *C. limicola* (Büttner et al., 1992) and PsaB sequences from *Synechocystis* 6803 (Smart & McIntosh, 1991), maize (Fish et al., 1985), and *C. reinhardtii* (Kück et al., 1987). The numbering is for PsaB from *C. reinhardtii*. Residues conserved in all sequences are bold. Potential membrane spanning regions are underlined. The F_X-binding domain is indicated.

To determine the importance of the helix X domain in coordinating P_{700}, site-directed mutants of H656 of PsaB have been constructed by genetic engineering of the chloroplast genome in *C. reinhardtii*. Previously, ENDOR spectroscopy has been employed successfully for the characterization of mutants directed to alter the primary donor, P_{865}, in bRC's of *Rhodobacter sphaeroides* (Huber et al., 1990; Rautter et al., 1995). These investigations revealed that changes in the surrounding protein environment have a dramatic impact on the spin density distribution in the cation radical $P_{865}^{+\bullet}$ and on the midpoint potential of $P_{865}^{+\bullet}$ (Lin et al., 1994). Here we describe mutations in PsaB that affect the oxidation midpoint potential, electronic structure, and optical properties of $P_{700}^{+\bullet}$. From the data we conclude that H656 of PsaB is close to and most likely a ligand to the central Mg atom of the spin carrying Chl of the P_{700} dimer in PSI.

METHODS

Site-Directed Mutagenesis and Chloroplast Transformation. The strategy for mutagenesis is outlined in Figure 2A. Plasmid pG528G is an *Eco*RI−*Pst*I fragment of chloroplast DNA that encodes the *psaB* gene and a portion of *rbcL* (Bingham et al., 1991). In addition, this plasmid contains a single silent site-directed mutation at codon position 528 that creates a unique *Stu*I site. The chimeric *aadA* (Goldschmidt-Clermont, 1991; Bingham & Webber, 1994) gene construct was cloned into a *Hin*cII site within the intergenic region between *psaB* and *rbcL* in pG528G to give plasmid pG528G-S. A *Bam*HI−*Pst*I fragment of pG528G was subcloned into M13mp19 and single-stranded DNA used as a template for oligonucleotide-directed mutagenesis. Following mutagenesis a *Stu*I−*Ban*II fragment was subcloned from M13 into pG528G-S and used in transformation experiments.

A PSII-minus mutant strain of *C. reinhardtii*, FuD7 (Bennoun et al., 1986), was used as the recipient of donor plasmids in the transformation experiments. The cells were maintained on HS medium supplemented with acetate (HSA) and spectinomycin (100 μg mL^{-1}) when required (Webber et al., 1993; Cui et al., 1995). Chloroplast transformation was performed by the biolistics technique as previously

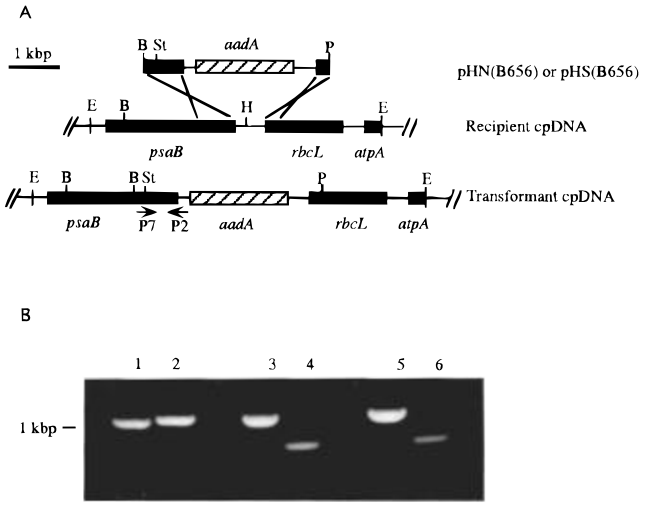

FIGURE 2: Chloroplast mutagenesis scheme and identification of segregated mutants by PCR. (A) Restriction enzyme map and chloroplast transformation strategy. The mutant plasmids pHN-(B656) and pHS(B656) contain a *Bam*HI−*Pst*I fragment of chloroplast restriction enzyme fragment *Eco*14. The plasmids contain mutations that produce the desired codon change and a silent mutation that introduces a new *Stu*I restriction enzyme cleavage site. The *aadA* gene was cloned into a *Hin*cII site located between *psaB* and *rbcL*. (B) A 1 kbp fragment of *psaB* was amplified by PCR (see Methods) from FuD7 (lane 1), HN(B656) (lane 3), and HS(B656) (lane 5) and digested with *Stu*I (lanes 2, 4, and 6).

described (Boynton et al., 1988; Webber et al., 1993). Bombarded cells were transferred to plates containing HSA supplemented with 100 μg mL^{-1} spectinomycin and 1.2% agar and placed under dim light for 7−10 days until colonies appeared. Single colonies were restreaked onto solid medium. Total DNA was isolated from cells taken from confluent regions of the plates as previously described (Webber et al., 1993) and resuspended at a final volume of 100 μL. One microliter of this DNA isolation was then used as a template for PCR using primers P2 and P7 (Figure 2A; Cui et al., 1995). To confirm the presence of the desired mutations the amplified DNA from the homoplasmic strains was sequenced using a Cycle Sequence kit (BRL) following the manufacturer's procedures.

PSI Isolation, Optical Spectroscopy, and Redox Titration. PSI complexes were isolated from thylakoid membranes as previously described (Cui et al., 1995). The flash-induced absorbance spectra were recorded using a laboratory-built flash spectrophotometer. The measuring light from a 55 W tungsten halogen lamp was passed through a monochromator with 3 nm bandwidth, a 1 cm optical cuvette, and a combination of interference and edge filter in front of the photomultiplier (EMI 9558BQ) that was coupled to a transient recorder (Tektronix TDS 320). The samples were excited by saturating Xe flashes of about 15 μs duration filtered by a colored glass (CS96-4 from Corning). Before measurements, the PSI complexes were diluted to approximately 10 μM Chl with a buffer containing 20 mM Tricine, pH 7.5, 25 mM $MgCl_2$, 0.02% *n*-dodecyl β-D-maltoside, 5 mM sodium ascorbate, and 10 μM phenazine methosulfate. The time course of the absorbance changes was fitted to an exponential decay using an algorithm that minimizes the sum of the unweighted least squares.

The midpoint potential of P_{700} was determined by measuring the magnitude of flash-induced absorbance increase at 826 nm, associated with oxidation of P_{700}, as a function of the redox potential poised in the reaction medium. Titrations were performed in a medium containing 25 mM PIPES, pH 6.8, 100 mM $MgCl_2$, 0.02% *n*-dodecyl β-D-maltoside, and approximately 20 μM Chl. The redox potentials of the solution were adjusted by additions of ferricyanide and ferrocyanide, respectively. The potentials were measured using platinum and calomel electrodes (Radiometer K4040 and P1040) connected to a Radiometer PHM82 pH meter.

EPR and ENDOR Spectroscopy. ENDOR was performed on the primary donor cation radical $P_{700}^{+\bullet}$ of PSI samples in frozen solution as previously described (Cui et al., 1993). P_{700} was oxidized optically by irradiating a concentrated PSI preparation in EPR quartz capillaries of 4 mm o.d. and 3 mm i.d. The Chl concentration for wild-type spectra was 4.0 mg mL^{-1} and for mutant spectra was 2 mg mL^{-1}. Illumination was performed at ambient temperature using a 1000 W tungsten lamp equipped with a water filter (10 cm path length) and an edge filter (665 nm Schott RG 665). After 1 min the samples were frozen under continued irradiation in liquid nitrogen and transferred to the spectrometer. The ENDOR measurements were performed on a Bruker ESP 300E X-band EPR spectrometer with home-built ENDOR accessories (Käss et al., 1994). A TM110-type microwave cavity/radiofrequency coil arrangement similar to that described in Zweygart et al. (1994) was used which provided a high *Q* factor (approximately 5000) resulting in a high ENDOR sensitivity. The sample temperature was controlled using a Bruker ER4111 VT nitrogen flow system.

RESULTS

Generation and Screening of Mutants in C. reinhardtii. We have transformed the chloroplast genome of *C. reinhardtii* to test the function of residue 656 in coordinating P_{700}. A fragment of the *psaB* gene was subjected to site-directed mutagenesis (Cui et al., 1995). Mutations were designed to change H656 to Ser or Asn. Substitution of His with Asn or Ser would provide either an alternative nitrogen or oxygen ligand to the central Mg^{2+} of Chl and may change properties of $P_{700}^{+\bullet}$ without major structural changes to the protein. Plasmids containing the mutations, and the selectable marker *aadA* cloned down stream of *psaB* (Figure 2), were used to transform the FuD7 mutant of *C. reinhardtii* by particle bombardment (Boynton et al., 1988; Webber et al., 1993). FuD7 lacks the PSII complex due to a deletion in the *psbA* gene and requires acetate as a reduced carbon source (Bennoun et al., 1986). Following transformation colonies were selected for spectinomycin resistance, indicating integration of *aadA* (Cui et al., 1995). The transforming plasmids also contained a silent mutation that introduced a unique *Stu*I site into *psaB* that could be used to screen for successful homologous replacement of the endogenous wild-type *psaB* gene by the mutated copies (Cui et al., 1995). PCR-amplified DNA from the transformants was digested with *Stu*I and size-fractionated by agarose gel electrophoresis. As shown in Figure 2B, the amplified DNA from each transformant could be completely digested with *Stu*I, indicating that chloroplast DNA was homoplasmic for the desired *psaB* mutations. Thylakoid membranes from the mutants and wild-type cells were found to contain similar amounts of PSI as determined from the polypeptide profiles following polyacrylamide gel electrophoresis (not shown).

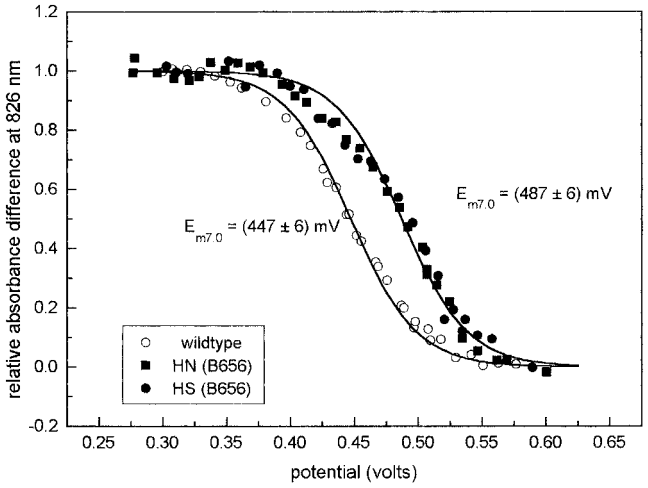

FIGURE 3: Redox titration of the flash-induced absorption change at 826 nm due to the formation of $P_{700}^{+\bullet}$ in PSI complexes of *C. reinhardtii*: (○) wild-type; (■) HN(B656); (●) HS(656S). The absorbance increase at 826 nm is attributed to formation of $P_{700}^{+\bullet}$. The solid lines represent one-electron Nernst curves with a midpoint potential of 445 and 488 mV for wild-type and mutants, respectively (vs NHE).

Optical Spectroscopy and Oxidation Midpoint Potential of $P_{700}/P_{700}^{+\bullet}$. To determine if the mutations affected the chemical properties of P_{700}, we measured the oxidation midpoint potential of $P_{700}/P_{700}^{+\bullet}$. The results of redox titrations of the flash-induced absorbance increase at 826 nm in PSI preparations of *C. reinhardtii* wild type and mutants HN(B656) and HS(B656) are shown in Figure 3 and Table 1. The solid lines represent one-electron ($n = 1$) Nernst curves. The midpoint potential of $P_{700}/P_{700}^{+\bullet}$ in the wild-type PSI preparation was determined as 447 ± 6 mV (vs NHE). In both mutants slightly better fits are obtained with $n = 0.8$, but this does not affect the result of the midpoint potentials. A slight heterogeneity was also noticed in the Nernst curves from the two mutants. Similar heterogeneity has also been noticed in other PSI mutants, such as HL-(B523) (Cui et al., 1995), that have an unaltered midpoint potential. In PSI from HN(B656) and HS(B656) the measured oxidation midpoint potential was increased to 487 ± 6 mV (Figure 3). These results indicate that the mutations

Table 1: Isotropic Methyl Proton Hyperfine Couplings of the Spin Carrying the Chl *a* Molecule of $P_{700}^{+\bullet}$ and Midpoint Potentials (vs NHE) for $P_{700}/P_{700}^{+\bullet}$ in PSI Prepared from *S. elongatus* and *C. reinhardtii*

species	A_{iso} (MHz)[a]			midpoint potential (mV)
	12[b]	7[b]	2[b]	
Synechococcus	5.25	3.51	2.89	436 ± 5
Chlamydomonas	5.32	3.65	2.93	445 ± 5
HS(B656)	6.09	3.65	3.00	488 ± 6
HN(B656)	6.32	3.76	3.01	487 ± 6

[a] Error of A_{iso} is ±0.05 MHz. [b] Molecular position to which the $A_{iso}(CH_3)$ is assigned in the spin carrying Chl *a* (Figure 6) of $P_{700}^{+\bullet}$.

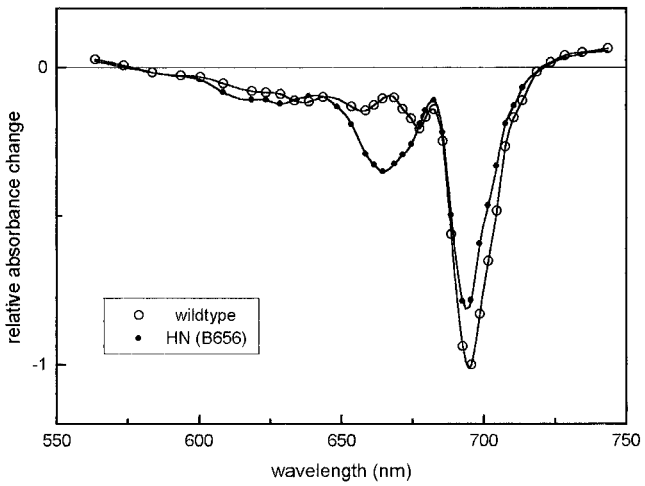

FIGURE 4: Flash-induced absorbance difference spectrum of $P_{700}/P_{700}^{+\bullet}$ measured at room temperature in PS I complexes of *C. reinhardtii*: wild-type (○) and mutant HN(B656) (●). The sample was excited by saturating Xe flashes of about 15 μs duration. The spectra are normalized to the same area under the curve in the Q_y region (between 650 and 720 nm).

have significantly altered the redox property of the PSI primary donor.

Further characterization of the mutants HN(B656) and HS(B656) was performed by absorbance difference spectroscopy. The spectra of the absorbance changes obtained from *C. reinhardtii* wild type and the mutant HN(B656) are shown in Figure 4. The difference spectrum measured with the mutant HS(B656) (not shown) was very similar to that of HN(B656). The spectra are normalized to the same bleached area between 650 and 720 nm (Q_y region) assuming that the total area due to the photooxidation of P_{700} is not changed by the mutations. The spectral features observed with PSI complexes from *C. reinhardtii* wild type agree well with those reported for the P_{700} difference spectrum measured in thylakoid membranes (Cui et al., 1995). The difference spectra are dominated by the main bleaching band that is centered at 696 nm in *C. reinhardtii* wild type and slightly blue shifted in the mutant. Low-temperature measurements with better spectral resolution ($\Delta\lambda = 1$ nm) indicate a blue shift of about 2−3 nm (not shown). Most interestingly, the difference spectra of both mutants also exhibit a pronounced new bleaching band at 667 nm indicating altered spectral properties of P_{700} induced by mutation of H(B656) to either Asn or Ser.

Electron Nuclear Double Resonance Spectroscopy of $P_{700}^{+\bullet}$. The oxidized primary donor $P_{700}^{+\bullet}$ in PSI isolated from wild type and mutants HN(B656) and HS(B656) has been characterized by EPR and ^{1}H ENDOR spectroscopy in

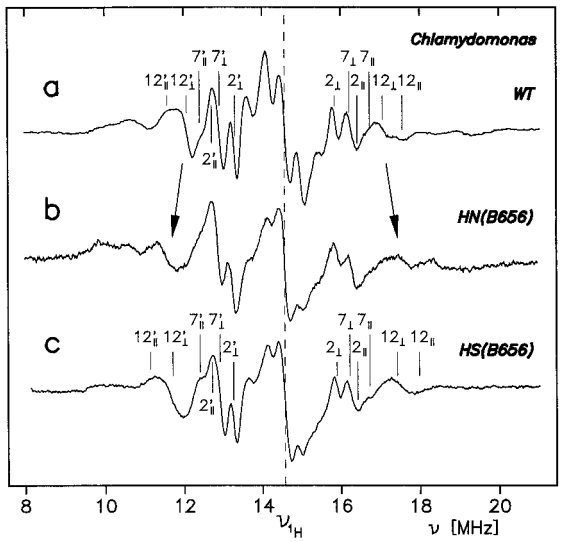

FIGURE 5: ^{1}H ENDOR (electron nuclear double resonance) spectra of $P_{700}^{+\bullet}$ in PSI from *C. reinhardtii* in frozen solution: (a) wild type at 160 K; (b) mutant HN(B656) at 160 K; (c) mutant HS(B656) at 160 K. The arrow indicates the shift of the lines belonging to the hfc at position 12 in the mutants.

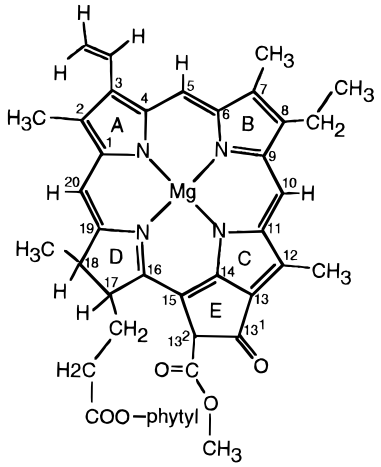

FIGURE 6: Molecular structure and IUPAC numbering scheme for chlorophyll *a* (Chl *a*).

frozen solution (120 K). For all preparations an unresolved Gaussian EPR line of 0.70 ± 0.01 mT was obtained at $g = 2.0025$ (not shown), indicating no major differences in the electronic state of $P_{700}^{+\bullet}$. The individual hfc's could be resolved by ENDOR spectroscopy. Figure 5 compares the powder-type spectra obtained for $P_{700}^{+\bullet}$ in wild type and the two mutants. The former spectrum has recently been analyzed in detail (Käss et al., 1995). Three axially symmetric ^{1}H hfc tensors could be assigned to the methyl groups at molecular positions 2, 7, and 12 (Figure 6) on the spin carrying Chl *a* half of $P_{700}^{+\bullet}$. The line positions of the parallel ($A_{||}$) and perpendicular ($A_\perp$) components of these three methyl group tensors are indicated in Figure 5a. The isotropic hfc's obtained by $A_{iso} = (1/3)(2A_\perp + 2A_{||})$ are given in Table 1. The hfc's are very similar to those obtained for $P_{700}^{+\bullet}$ in PSI of spinach and *S. elongatus* (Käss, 1995). The ^{1}H ENDOR spectrum of $P_{700}^{+\bullet}$ from the mutant HN(B656) is distinctly different from that of the wild type. In particular, the hfc assigned to the methyl group at position 12 is increased by about 20%. This hfc is also larger (approximately 16%) for the HS(B656) mutant. The methyl group hfc's at positions 2 and 7 do not show a significant

increase in magnitude. Due to the strongly asymmetric spin density distribution of approximately 85:15 (Käss, 1995; Käss et al., 1995) over the dimer halves in $P_{700}^{+\bullet}$, only changes of the large hfc's of the Chl *a* carrying the majority of the spin density are easily detected in the ^{1}H ENDOR spectra. However, the spectra (Figure 5) also indicate shifts and intensity changes of the smaller couplings which might be attributed to the second dimer half. The result obtained here clearly shows that mutations at position B656 significantly disturb the spin density of $P_{700}^{+\bullet}$, indicating a close contact between this histidine residue and the primary donor in wild-type PSI.

DISCUSSION

Mutation of His-656 of the PsaB RC protein to either Asn or Ser results in an increase in the oxidation midpoint potential of $P_{700}/P_{700}^{+\bullet}$ by approximately 40 mV. Both mutations also lead to an increase of the methyl proton hfc's, in particular at molecular position 12 of the spin carrying Chl *a*. This clearly shows that the mutations HN(B656) and HS(B656) induce an alteration of the environment of $P_{700}^{+\bullet}$ in a manner not observed in any other PsaB mutations characterized so far (Cui et al., 1995). This indicates that H(B656) must interact closely with one Chl *a* of the P_{700} dimer. This conclusion is supported by the altered spectral properties of P_{700} due to the mutation of H(B656) to either Asn or Ser. Assuming that the bleached areas in the Q_y region (corresponding to the oscillatory strength expected for the oxidation of P_{700}) are the same in the wild type and in the mutants, analysis of the so normalized spectra indicates that the intensity of the main bleaching around 695 nm decreases and a new bleaching band centered around 667 nm appears. Furthermore, the main bleaching band is slightly blue shifted in the mutants. The flash-induced absorbance changes are suppressed in the presence of ferricyanide, which blocks photochemistry of PSI by chemical oxidation of P_{700}. One possible explanation of the significantly changed spectral characteristics of P_{700} would be that a neighboring Chl absorbing around 667 nm is oxidized by $P_{700}^{+\bullet}$ as a consequence of its increase in oxidation midpoint potential in the mutants. An equilibrium level of about 3 for the reaction P_{700}^{+}Chl $\leftrightarrow$ P_{700}Chl^{+} can be roughly estimated from the bleached areas. The ENDOR spectra show no indication of a cation radical different from $P_{700}^{+\bullet}$; however, it is sometimes difficult to detect low levels ($\leq$25% in this case) of a secondary radical in such an overcrowded spectrum. Alternatively, the differences between the $P_{700}/P_{700}^{+\bullet}$ spectra may indicate an altered excitonic interaction between the two Chl *a* molecules of P_{700} induced by the mutations. On the basis of simple exciton theory, the 667 nm band may be assigned to the high-energy exciton component of P_{700} in the mutants (Cantor & Schimmel, 1980). Using the point−dipole approximation, this corresponds to an exciton interaction energy of about 290 cm^{-1} and an angle of about 60° between the Q_y transitions of the two Chl *a* molecules of the P_{700} dimer calculated from the estimated ratio of the oscillator strengths of the 667 and 695 nm band of approximately 1:3 (Cantor & Schimmel, 1980). In wild-type PSI, the position of the high-energy exciton component of P_{700} is not clearly seen due to its small oscillator strength, indicating a more parallel orientation of the Chl Q_y transitions (Setif, 1992). If the ratio of the oscillator strengths is estimated to be $\leq$1:10 in the wild type, it results in an angle of $\leq$35° similar to that of the special pair of pigments in purple bacteria (38°). Even though the spectral properties of P_{700} in wild type and in mutants are not well understood, it seems reasonable that small changes in geometry within the dimer can account for the observed spectral changes of the primary donor.

Several mechanisms can affect the oxidation midpoint potential together with the spin density distribution and the optical properties of $P_{700}^{+\bullet}$. First, it is possible that His-656 of the PsaB protein forms a hydrogen bond to the keto carbonyl group of one of the Chl *a* molecules in P_{700}. Removal and/or addition of hydrogen bonds to 3 and 13^1 carbonyl groups of the BChl *a* dimer in $P_{865}^{+\bullet}$ in ring A (acetyl) or ring E (keto) has been shown to affect both redox and electronic properties of the oxidized primary donor in *R. sphaeroides* (Rautter et al., 1995; Lin et al., 1994, Allen & Williams, 1995). Generating a new hydrogen bond to the 13^1-keto carbonyls by changing a Leu to His at position L131 of the L protein subunit [mutant LH(L131)], or at position M160 of the M subunit [mutant LH(M160)], raised the oxidation midpoint potential of $P_{865}/P_{865}^{+\bullet}$ by approximately 50−60 mV (Lin et al., 1994). With respect to the electronic structure of $P_{865}^{+\bullet}$ these mutations influenced all hfc's of both Bchl halves by shifting the spin density from one to the other dimer half in $P_{865}^{+\bullet}$ (Rautter et al., 1995). If His(B656) would form such a hydrogen bond to the keto group of one of the P_{700} Chl's, the weakening of the hydrogen bond by substitution with Ser or Asn should decrease the redox potential. What we observe is an increase of about 40 mV in both mutants HN(B656) and HS(B656). Therefore, it is unlikely that such a hydrogen bond is formed.

Second, the introduction of charged amino acid residues in the bRC protein in the vicinity of the P_{865} can result in a change of the midpoint oxidation potential by electrostatic interactions (Allen & Williams, 1995). In the RC of *Rb. capsulatus* the mutation YH(M210) decreased the oxidation potential of $P_{865}/P_{865}^{+\bullet}$ by approximately 36 mV (Jia et al., 1993). The distance of Tyr M210 to the special pair is about 5 Å, which does not allow the formation of hydrogen bonds. The reverse case, i.e., the exchange of His by another amino acid residue, would be expected to result in an increase of the redox potential, as is observed here. However, in this situation the hfc's of $P_{700}^{+\bullet}$ should all be altered almost equally to a minor extent instead of showing a pronounced specific increase of one hfc at a particular position as we observe for the mutations HS(B656) and HN(B656).

Finally, His at position 656 could be an axial ligand to the central Mg atom of one of the Chl *a* molecules in the dimer P_{700}. In the bRC of *Rb. sphaeroides* the substitution of His M202 or His L173 causes removal of the Mg atom of the neighboring BChl *a* if the substitution is by a voluminous amino acid like Leu or Phe. This leads to the so-called heterodimer with one BChl and one BPhe (Bylina & Youvan, 1988). In the mutant HL(M202) the oxidation potential is increased by 160 mV as compared to wild type. This is the largest effect on potential observed by any single RC mutation (Allen & Williams, 1995). As compared with the wild-type bRC the HL(M202) mutation produces significant changes in absorption, EPR, and ENDOR spectra (Rautter et al., 1995; Kirmaier et al., 1988; Bylina et al., 1990; Huber & Törring, 1995). The spin is localized on the BChl *a* half of the oxidized bRC (BChl/BPheo) heterodimer. In case of P_{700} in PSI the mutation HL(B656) may similarly

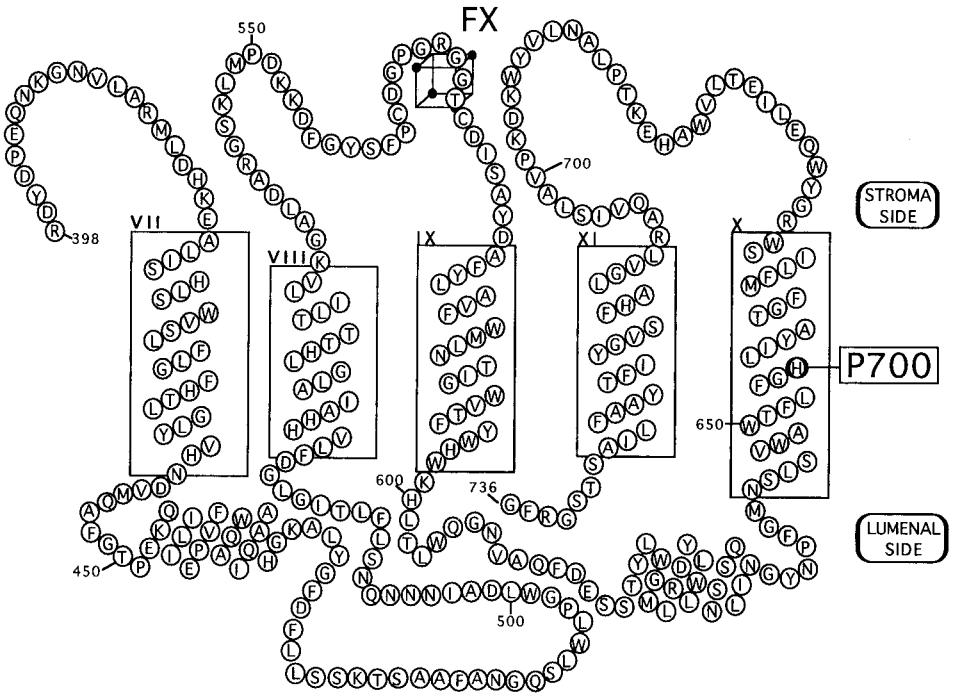

FIGURE 7: Model of the coordination of PSI cofactors by helices VII−XI of PsaB. The amino acid sequence and numbering are derived from analysis of the *psaB* gene from *C. reinhardtii* (Kück et al., 1987).

result in the formation of a heterodimer (Chl *a*/Phe *a*) in analogy to the bRC. But unlike in the bacteria, where the mutations HL(M202) and HL(L173) influence the stability of the bRC's only to a minor extent (Bylina & Youvan, 1988), this mutant assembles only low amounts of PSI (data not shown). The same phenomenon was observed in PSII where the exchange of the predicted P_{680} Mg coordinating His to Leu (His-198 in D1 and His-197 in D2) leads to PSII complexes that are not stably assembled (Nixon et al., 1992).

Assuming that His(B656) is a ligand to the Mg of the spin carrying Chl *a* in the primary donor, the mutations HN(B656) and HS(B656) would probably not lead to a removal of the central Mg atom since Asn and Ser are considerably smaller than Leu and also can still ligate the Mg. However, the smaller volume and shorter length of the amino acids introduced by the mutations at position B656 may lead to changes in the geometry of the Chl *a* dimer, as suggested by the changes in the absorption difference spectra. This may also influence the redox properties of $P_{700}/P_{700}^{+\bullet}$. Investigations of substituted monomeric Chl *a* molecules have shown that the redox potential is dependent on steric effects and is particularly sensitive to strain in ring E of the molecule (Heald & Cotton, 1990). The redox potential is increased from +540 mV in Chl *a* to +650 mV in 13^2-hydroxy-Chl *a*, in clear contrast to the expected inductive effect of the electron-donating OH group that should cause a decrease of the potential. This was rationalized by assuming an increased steric strain of ring E in 13^2-hydroxy-Chl *a*, due to the more voluminous OH group. The assumption of such steric effects in Chl *a*-type systems is corroborated by comparative ENDOR studies of substituted BChl *a* cations which revealed a steric effect due to substituents at position 13 in the BChl *a* molecule (Käss et al., 1994).

Substitution with Gln and Gly at position M202 or Gly at position L173 in *Rb. sphaeroides* RC does not lead to formation of a heterodimer. In the HG(M202) and HG-(L173) mutants the central Mg is coordinated by an adventitious ligand, speculated to be water, and the midpoint potential of the donor is unchanged (Goldsmith et al., 1996). The oxidation potential in the HQ(M202) mutant is unknown. The ENDOR characterization of the HG(L173) mutant revealed that the hfc's are changed in an identical manner to those in the PsaB mutants described here (unpublished observations). Only the coupling of the methyl protons at position 12 of the BChl is affected whereas the coupling at position 2 remains almost constant. The increase of this coupling (position 12) is about 15%. This influences the electronic structure leading to the different spin distribution that is clearly observable in the ENDOR spectrum. This result indicates that it is possible to affect the spin distribution in a very localized manner by altering an axial ligand to one chlorophyll of the primary donor.

In summary, we conclude that His-656 of PsaB is in close proximity to the spin carrying Chl *a* of $P_{700}^{+\bullet}$. Based on the above discussion the most likely explanation for the significantly changed properties of P_{700} in the mutants HN(B656) and HS(B656) is that the His at position B656 of PSI coordinates the central Mg atom of the spin carrying half of $P_{700}^{+\bullet}$. However, further analysis of additional mutations at this position and at the equivalent His in the PsaA subunit is required to confirm this. His-656 is located toward the center of the predicted membrane span X of PsaB, which is difficult to reconcile with the location of P_{700} toward the lumenal side of PSI. In the *H. mobilis* RC primary sequence a Pro and Lys are found 5 and 6 amino acids toward the lumenal side of the helix X His, which might suggest that His-656 is indeed located closer to the lumenal side of the complex. However, this discussion is based solely on predicted hydrophobicity profiles and awaits direct determination from a higher resolution structure.

The current 4.5 Å structure of PSI indicates that two symmetrical helices, e and e′, are close to electron densities attributed to the P_{700} chlorophyll dimer (Schubert et al.,

1995). Our results show that helix X of PsaB interacts closely with P_{700}, suggesting that it corresponds to helix e or e′ observed in the 4.5 Å structure, renamed m and m′ in the 4 Å model (Wolf-Dieter Schubert, personal communication). It has previously been noted that there is a strikingly similar organization of the cofactors in both the type I and type II RCs (Golbeck, 1993). Since the amino acid sequence homology between type I and type II RCs is low, it was never possible to draw any firm conclusions. However, even with low amino acid identity it might be expected that protein domains coordinating the cofactors in type I and type II RC's may have been retained during the course of evolution. Our results indicate that the helix X region of PsaB is closely associated with the P_{700} RC Chl *a*. On the basis of these data we propose a model for coordination of PSI cofactors shown in Figure 7. In this model, the C-terminal five helices of the PsaB protein coordinate the F_X [4Fe-4S] iron−sulfur center and the primary donor (Figure 7) in a manner analogous to helices A through E of the type II RC. Helix X of PsaB plays a role identical to helix D of the D1 and D2 polypeptides of PSII and the L and M subunits of purple bacteria. Vermaas (1994) has previously reported significant homology between helices I−VI of the RC protein of *H. mobilis* and the CP43 antenna protein of PSII, which also has six transmembrane spans. Thus, a model in which the first six membrane spans of PsaB constitute an antenna domain and the last five membrane spans the RC domain is further supported by these results.

ACKNOWLEDGMENT

We thank the *Chlamydomonas* Genetics Center at Duke University for providing plasmids and cultures.

REFERENCES

Allen, J. P., & Williams, J. C. (1995) *J. Bioenerg. Biomemb. 27*, 275−283.
Allen, J. P., Feher, G., Yeates, I. O., Komiya, H., & Rees, D. C. (1987) *Proc. Natl. Acad. Sci. U.S.A. 84*, 5730.
Bennoun, P. M., Spierer-Herz, J., Erickson, J., Girard-Bascou, J., Pierre, Y., Delsome, M., & Rochaix, J.-D. (1986) *Plant Mol. Biol. 6*, 151−160.
Bingham, S. E., & Webber, A. N. (1994) *J. Appl. Phycol. 6*, 239−245.
Bingham S. E., Xu, R., & Webber A. N. (1991) *FEBS Lett. 292*, 137−140.
Boynton, J. E., Gillham, N. W., Harris, E. H., Hosler, J. P., Johnson, A. M., Jones, A. R., Randolph-Anderson, B. L., Robertson, D., Klein, T. M., Shark, K. B., & Sanford, J. C. (1988) *Science 240*, 1534−1538.
Büttner, M., Xie, D.-L., Nelson, H., Pinther, W., Hauska, G., & Nelson, N. (1992) *Proc. Natl. Acad. Sci. U.S.A. 89*, 8135−8139.
Bylina, E. J., & Youvan, D. C. (1988) *Proc. Natl. Acad. Sci. U.S.A. 85*, 7226−7230.
Bylina, E. J., Kolaczkowski, S. V., Norris, J. R., & Youvan, D. C. (1990) *Biochemistry 29*, 6203−6210.
Cantor, C. R., & Schimmel, P. R. (1980) *Biophysical Chemistry Part II: Techniques for the Study of Biological Structure and Function*, pp 349−408, W. H. Freeman, San Francisco, CA).
Chang, C.-H., El-kabanni, O., Tiede, D., Norris, J., & Schiffer, M. (1991) *Biochemistry 30*, 5352−5360.
Cui, L., Bingham. S. E., Kuhn, M., Käss, H., Lubitz, W., & Webber, A. N. (1995) *Biochemistry 34*, 1549−1558.
Deisenhofer, J., Epp, O., Mikki, K., Huber, R., & Michel, H. (1984) *J. Mol. Biol. 180*, 385.
Ermler, U., Fritzsch, G., Buchanan, S. K., & Michel, H. (1994) *Structure 2*, 925−936.
Fish, L. E., Kück, U., & Bogorad, L. (1985a) *J. Biol. Chem. 260*, 1413−1419.
Fish, L. E., Kück,.U., & Bogorad, L. (1985b) in *Molecular Biology of the Photosynthetic Apparatus* (Steinback, K. E., Bonitz, S., Arntzen, C. J., & Bogorad, L., Eds.) pp 111−120, Cold Spring Harbor Laboratory Press, Cold Spring Harbor, NY.
Fromme, P., Schubert, W.-D., & Kraub, N. (1994) *Biochim. Biophys. Acta 1187*, 99−105.
Golbeck, J. H. (1993) *Proc. Natl. Acad. Sci. U.S.A. 90*, 1642−1646.
Golbeck, J. H. (1992) *Annu. Rev. Plant Physiol. Plant Mol. Biol. 43*, 293−324.
Goldschmidt-Clermont, M. (1991) *Nucleic Acids Res. 19*, 4083−4089.
Goldsmith, J. O., King, B., & Boxer, S. G. (1996) *Biochemistry 35*, 2421−2428.
Heald, R. L., & Cotton, T. M. (1990) *J. Phys. Chem. 94*, 3968−3975.
Huber, M., & Törring, J. T. (1995) *Chem. Phys. 194*, 379−385.
Huber, M., Lous, E. J., Isaacson, R. A., Feher, G., Gaul, D., & Schenck, C. C. (1990) in *Reaction Centers of Photosynthetic Bacteria* (Michel-Beyerle, M. E., Ed.) pp 219−228, Springer Verlag, Berlin.
Jia, Y., DiMagno, T. J., Chan, C.-K., Wang, Z., Du, M., Hanson, D. K., Schiffer, M., Norris, J. R., Fleming, G. R., & Popov, M. S. (1993) *J. Phys. Chem. 97*, 13180−13191.
Käss, H. (1995), Ph.D. Thesis, Technische Universität Berlin.
Käss, H., Rautter, J., Zweygart, W., Struck, A., Scheer, H., & Lubitz, W. (1994) *J. Phys. Chem. 98*, 354−363.
Käss, H., Bittersmann-Weidlich, E., Andréasson, L.-E., Bönigk, B., & Lubitz, W. (1995) *Chem. Phys. 194*, 419−432.
Kirmaier, C., Holten, D., Bylina, E. J., & Youvan, D. C. (1988) *Proc. Natl. Acad. Sci. U.S.A. 85*, 7562−7566.
Kück, U., Choquet, Y., Schneider, M., Dron, M., & Bennoun, P. (1987) *EMBO J. 6*, 2185−2192.
Liebl, U., Mockensturn-Wilson, M., Trost, J. T., Brune, D. C., Blankenship, R. E., & Vermaas, W. (1993) *Proc. Natl. Acad. Sci. U.S.A. 90*, 7124−7128.
Lin, X., Murchison, H. A., Nagarajan, V., Parson, W. W., Allen, J. P., & Williams, J. C. (1994) *Proc. Natl. Acad. Sci. U.S.A. 91*, 10265−10269.
Marguilles M. M. (1991) *Photosynth. Res. 29*, 133−147.
Nixon, P. J., Chisholm, D. A., & Diner, B. (1992) in *Plant Protein Engineering* (Shewry, P. R., & Gutteridge, S., Eds.) pp 93−142, Cambridge University Press, Cambridge, U.K.
Rautter, J., Lendzian, F., Schulz, C., Fetsch, A., Kuhn, M., Lin, X., Williams, J. C., Allen, J. P., & Lubitz, W. (1995) *Biochemistry 34*, 8130−8143.
Schubert, W. D., Klukas, O., Krauss, N., Saenger, W., Fromme, P., & Witt, H. T. (1995) in *Photosynthesis: From Light to Biosphere* (Mathis, P., Ed.) Vol. II, pp 3−11, Kluwer Academic Press, Amsterdam, The Netherlands.
Setif, P. (1992) in *The Photosystems: Structure, Function and Molecular Biology* (Barber, J., Ed.) pp 471−499, Elsevier, New York.
Smart, L. B., & McIntosh, L. (1991) *Plant Mol. Biol. 17*, 959−969.
Smart, L. B., Warren, P. V., Golbeck, J. H., & McIntosh, L. (1993) *Proc. Natl. Acad. Sci. U.S.A. 90*, 1132−1136.
Vermaas W. F. J. (1994) *Photosynth. Res. 41*, 285−294.
Webber, A. N., Gibbs, P. B., Ward, J. B., & Bingham, S. E. (1993) *J. Biol. Chem. 268*, 12990−12995.
Zweygart, W., Thanner, R., & Lubitz, W. (1994) *J. Magn. Reson. A 109*, 172−176.

BI961198W